

# Experimental realization of a quantum algorithm

Isaac L. Chuang<sup>1</sup>, Lieven M.K. Vandersypen<sup>2</sup>, Xinlan Zhou<sup>2</sup>, Debbie W. Leung<sup>3</sup>, and Seth Lloyd<sup>4</sup>

<sup>1</sup> IBM Almaden Research Center K10/D1, San Jose, CA 95120, <sup>2</sup> Solid State Electronics Laboratory, Stanford University, Stanford, CA 94305

<sup>3</sup> Edward L. Ginzton Laboratory, Stanford University, Stanford, CA 94305 <sup>4</sup> MIT Dept. of Mechanical Engineering, Cambridge, Mass. 02139

submitted January 19, 1998; revised March 7, 1998, accepted March 18, 1998.

A quantum computer is a device that processes information in a quantum-mechanically coherent fashion<sup>1-5</sup>. In principle, it can exploit coherent quantum interference and entanglement to perform computations, such as factoring large numbers or searching an unsorted database, more rapidly than classical computers<sup>1,2,6-8</sup>. Noise, decoherence, and manufacturing problems make constructing large-scale quantum computers difficult<sup>9-13</sup>. Ion traps and optical cavities offer promising experimental approaches<sup>14,15</sup>, but no quantum algorithm has yet been implemented with those systems. On the other hand, because of their natural isolation from the environment, nuclear spins are particularly good ‘quantum bits’<sup>16</sup>, and their use for quantum computation is possible by applying nuclear magnetic resonance (NMR) techniques in an unconventional manner<sup>17-19</sup>. Here, we report on the experimental realization of a quantum algorithm using NMR, to solve a purely mathematical problem in fewer steps than is possible classically. In particular, our simple quantum computer can determine global properties of an unknown function using fewer function ‘calls’ than is possible using a classical computer.

We implemented the simplest possible version of the Deutsch-Jozsa (D-J) quantum algorithm<sup>6</sup>, which determines whether an unknown function is constant or balanced. A constant function  $f(x)$  from  $N$  bits to one bit either has output  $f(x) = 0$  for all  $x$ , or  $f(x) = 1$  for all  $x$ . A balanced function has  $f(x) = 0$  for exactly half of its inputs, and  $f(x) = 1$  for the remaining inputs. To determine with certainty whether a function is constant or balanced on a deterministic classical computer, requires up to  $2^{N-1} + 1$  function calls: even if one has looked at half of the inputs and found  $f(x) = 0$  for each, one still can’t conclude with certainty that the function is constant. In contrast, the D-J algorithm, as improved by R. Cleve, et al.<sup>20</sup> and Alain Tapp, allows a quantum computer to determine whether  $f(x)$  is constant or balanced using only one function call.

The D-J algorithm is well illustrated by its simplest possible case, when  $f$  is a function from one bit to one bit; this is the version that we have realized (it is also the simplest instance of Simon’s algorithm<sup>7</sup>). There are four possible  $f$ ’s, two of which are constant,  $f_1(x) = 0$ ,  $f_2(x) = 1$  and two of which have an equal number of 0 and 1 outputs:  $f_3(x) = x$ ,  $f_4(x) = \text{NOT } x$ . To determine whether such a function is constant or balanced is analogous to determining whether a coin is fair – with heads on one side and tails on the other; or fake – with heads on both sides. Classically, one must look at the coin twice, first one side then the other, to determine if it is fair

or fake. The D-J algorithm exploits quantum coherence to determine if a quantum ‘coin’ is fair or fake while looking at it only once. The algorithm requires one ‘input’ spin and one ‘work’ spin, and is schematically represented by the quantum circuit shown in Fig. 1.

Experimentally, this quantum algorithm was implemented using the nuclear spins of the <sup>1</sup>H and <sup>13</sup>C atoms in a carbon-13 labeled chloroform molecule (CHCl<sub>3</sub>) as the input and work quantum bits (‘qubits’).  $|0\rangle$  ( $|1\rangle$ ) describes the spin state aligned with (against) an externally applied, strong static magnetic field  $\mathbf{B}_0$  in the  $+\hat{z}$  direction. The reduced Hamiltonian for this 2-spin system is to an excellent approximation given by ( $\hbar = 1$ )<sup>21</sup>

$$\hat{H} = -\omega_A \hat{I}_{zA} - \omega_B \hat{I}_{zB} + 2\pi J \hat{I}_{zA} \hat{I}_{zB} + \hat{H}_{env}. \quad (1)$$

The first two terms describe the free precession of spin  $A$  (<sup>1</sup>H) and  $B$  (<sup>13</sup>C) about  $-\mathbf{B}_0$  with frequencies  $\omega_A/2\pi \approx 500$  MHz and  $\omega_B/2\pi \approx 125$  MHz.  $\hat{I}_{zA}$  is the angular momentum operator in the  $+\hat{z}$  direction for  $A$ . The third term describes a scalar spin-spin coupling of the two spins of  $J \approx 215$  Hz.  $\hat{H}_{env}$  represents couplings to the environment, including interactions with the chlorine nuclei, and also higher order terms in the spin-spin coupling, which can be disregarded (as will be described below).

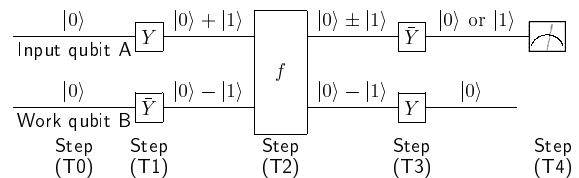


FIG. 1. Quantum circuit for performing the D-J algorithm. **(T0)** Start with both the ‘input’ and ‘work’ qubits ( $A$  and  $B$ ) in the state  $|0\rangle$ . **(T1)** Perform the transformation  $Y:|0\rangle \rightarrow (|0\rangle + |1\rangle)/\sqrt{2}$ ,  $|1\rangle \rightarrow (-|0\rangle + |1\rangle)/\sqrt{2}$ , to  $A$ , and the inverse transformation  $\bar{Y}$  to  $B$ , resulting in the state  $\frac{1}{2} \sum_{x=0}^1 |x\rangle (|0\rangle - |1\rangle)$ . The input qubit in some quantum sense registers both 0 and 1 at once. **(T2)** Call the function: apply  $f$  to  $A$ , and add the result to  $B$  modulo 2. As long as the quantum logic operations needed to evaluate  $f$  are carried out coherently, the work qubit now contains in some quantum sense the outputs of  $f$  on all possible inputs, an effect that Deutsch termed ‘quantum parallelism’<sup>1</sup>. The two qubits are now in the state  $\frac{1}{2} \sum_{x=0}^1 |x\rangle (|0 + f(x)\rangle - |1 + f(x)\rangle) = \frac{1}{2} \sum_{x=0}^1 (-1)^{f(x)} |x\rangle (|0\rangle - |1\rangle)$ . **(T3)** Perform the inverse of the transformations of **(T1)**, thereby taking the qubits out of their superposition states. If  $f$  is constant, then the factors  $(-1)^{f(x)}$  are either all  $+1$  or all  $-1$ , and the result of the transformation in this step is the state  $\pm|00\rangle$ . If  $f$  is balanced, then exactly half of the factors  $(-1)^{f(x)}$  are  $+1$  and half are  $-1$ , and the result of the transformation is the state  $\pm|10\rangle$ . **(T4)** Read out  $A$ . If it is 0, then  $f$  is constant; if it is 1, then  $f$  is balanced.

The five theoretical steps of the quantum algorithm, **(T0)**–**(T1)**, were experimentally implemented as follows:

**(E0)** An input state is prepared with a 200 mM, 0.5 ml sample of chloroform dissolved in d<sub>6</sub>-acetone, at room temperature and standard pressure. The  $\mathcal{O}(10^{18})$  molecules in this

bulk sample can be thought of as being independent single quantum computers, all functioning simultaneously. The theoretically ideal result is obtained when the spins in all the molecules start out in the 00 state. Because the experiment is performed at room temperature, however, the initial density matrix  $\rho$  for the thermally equilibrated system has populations  $\text{diag}(\rho) = [n_{00}, n_{01}, n_{10}, n_{11}]$  in the 00, 01, 10, and 11 states, respectively, where  $\rho$  is the density matrix, and  $n_i$  are proportional to  $e^{-E_i/kT}/2^N \approx (1 - E_i/kT)/2^N$ , with  $E_i$  the energy of state  $i$  and  $N = 2$  being the number of qubits used in our experiment. A variety of techniques exist to extract from this thermal state just the signal from the 00 state<sup>17,18</sup>; we adopted the method of ‘temporal averaging’<sup>22</sup>, which involves the summation of three experiments in which the populations of the 01, 10, and 11 states are cyclically permuted before performing the computation. The essential observation is that  $[n_{00}, n_{01}, n_{10}, n_{11}] + [n_{00}, n_{11}, n_{01}, n_{10}] + [n_{00}, n_{10}, n_{11}, n_{01}] = \alpha[1, 1, 1, 1] + \delta[1, 0, 0, 0]$ , where  $\alpha = n_{01} + n_{10} + n_{11}$  is a background signal which is not detected, and  $\delta = 3n_{00} - \alpha$  is a deviation from the uniform background whose signal behaves effectively like the desired pure quantum state,  $|00\rangle$ . The permutations are performed using methods similar to those used for the computation, described next. This technique avoids the technical difficulties of detecting the signal from a single nuclear spin, and allows a sample at room temperature, which produces an easily detectable signal, to be used for quantum computation.

Note that while this method requires  $f(x)$  to be evaluated 3 times, it is actually not necessary. Although step (T0) stipulates an input pure state  $|00\rangle$ , the algorithm works equally well if the input qubit is initially  $|1\rangle$ ; furthermore, when the work qubit is initially  $|1\rangle$ , it fails, and cannot distinguish constant from balanced functions, but this does not interfere with other computers which have worked. Thus, a thermal state is a good input for this algorithm, and only one experiment needs to be performed. Data from both thermal and pure state inputs are presented below.

**(E1)** Pulsed radio frequency (RF) electromagnetic fields are applied to transform the qubits as prescribed in (T1). These fields, oriented in the  $\hat{x} - \hat{y}$  plane perpendicular to  $\mathbf{B}_0$ , selectively address either  $A$  or  $B$  by oscillating at frequency  $\omega_A$  or  $\omega_B$ . Classically, an RF pulse along  $\hat{y}$  (for example) rotates a spin about that axis by an angle proportional to  $\approx tP$ , the product of the pulse duration  $t$  and pulse power  $P$ . In the ‘bar magnet’ picture, a  $\pi/2$  pulse along  $\hat{y}$  (we shall call this  $Y$ ) causes a  $\hat{z}$  oriented spin to be rotated by  $90^\circ$ , onto  $\hat{x}$  (similarly, we shall let  $\bar{Y}$  denote  $\pi/2$  rotations about  $-\hat{y}$ , and  $X$  denote  $\pi/2$  rotations about  $\hat{x}$ , and so forth; subscripts will identify which spin the operation acts upon). This description of the state is classical in the sense that a bar magnet always has a definite direction. In reality, however, a nuclear spin is a quantum object, and instead of being aligned along  $\hat{x}$ , it is actually in a superposition of being up and down,  $(|0\rangle + |1\rangle)/\sqrt{2}$ . Likewise, a spin classically described as being along  $-\hat{x}$  is actually in the state  $(|0\rangle - |1\rangle)/\sqrt{2}$ . (E1) thus consists of applying the two RF pulses  $Y_A\bar{Y}_B$ .

**(E2)** The function  $y \rightarrow y \oplus f(x)$  is implemented using RF pulses and spin-spin interaction. Recall that spin  $A$  represents the input qubit  $x$ , and  $B$  the work qubit  $y$  where  $f$  stores its output.  $f_1$  is implemented as  $\tau/2 - X_B X_B - \tau/2 - X_B X_B$ , to be read from left to right, where  $\tau/2$  represents a time interval

of  $1/4J \approx 1.163$  ms, during which coupled spin evolution occurs. Dashes are for readability only, and typical pulse lengths were 10-15  $\mu\text{s}$ . This is a well known refocusing<sup>23</sup> pulse sequence which performs the identity operation.  $f_2$  is  $\tau/2 - X_B X_B - \tau/2$ , similar to  $f_1$  but without the final pulses, so that  $B$  is inverted.  $f_3$  is  $Y_B - \tau - \bar{Y}_B X_B - \bar{Y}_A \bar{X}_A Y_A$ , which implements a ‘controlled-NOT’ operation, in which  $B$  is inverted if and only if  $A$  is in the  $|1\rangle$  state. The naive ‘bar magnet’ picture can be used to get a feeling for how this works in case the inputs are 00 or 10, for which the subsequence  $Y_B - \tau - X_B$  suffices (note that after (E1), both spins are not just  $|0\rangle$  or  $|1\rangle$  but in a superposition of both, in which case the extra pulses of  $f_3$  are necessary<sup>17</sup>). First,  $Y_B$  rotates  $B$  to  $+\hat{x}$ .  $B$  then precesses in the  $\hat{x} - \hat{y}$  plane, about  $-\hat{z}$ . Due to the spin-spin coupling,  $B$  precesses slightly slower (faster) if  $A = 0$  ( $A = 1$ ). After  $\tau$  seconds,  $B$  reaches  $+\hat{y}$  ( $-\hat{y}$ ) in the rotating frame.  $X_B$  then rotates  $B$  to  $+\hat{z}$  ( $-\hat{z}$ ), i.e. to 0 or 1, where the final state of  $B$  depends on the input  $A$ . The precise quantum description is easily obtained by multiplying out the unitary rotation matrices. Finally,  $f_4$  is implemented as  $Y_B - \tau - \bar{Y}_B \bar{X}_B - \bar{Y}_A \bar{X}_A Y_A$ , which is similar to  $f_3$  but leaves  $B$  inverted.

**(E3)** The inverse of (E1) is done by applying the RF pulses  $\bar{Y}_A Y_B$  to take both spins back to  $\pm\hat{z}$ . Spin  $A$ , which was  $|0\rangle$  at the input, is thus transformed into  $|0\rangle$  or  $|1\rangle$  for constant or balanced functions respectively.

**(E4)** The result is read out by applying a read-out pulse  $X_A$  to bring spin  $A$  back into the  $\hat{x} - \hat{y}$  plane. The time varying voltage  $V(t)$  induced by the precession of spin  $A$  about  $-\mathbf{B}_0$  is recorded by a phase sensitive pick-up coil. Inspection of the spectrum of  $V(t)$  after a single experiment run and an appropriate read-out pulse, immediately reveals whether  $f(x)$  is constant or balanced, as shown in Fig. 2.

We also characterized the entire deviation density matrix  $\rho_\Delta \equiv \rho - \text{Tr}(\rho)I/4$  (Fig. 3) describing the final 2-qubit state. These results unambiguously demonstrate the complete proper functioning of the quantum algorithm, and provide data for the error analysis described below.

Quantum computation requires that a coherent superposition be preserved for the duration of the computation. This requires a highly isolated quantum system (small  $\mathcal{H}_{env}$ ), and fortunately, nuclear spins are naturally well-isolated from their environment. Phase randomization due to  $\mathbf{B}_0$  inhomogeneities was minimized by using about 30 electromagnetic coils to shim the static field to be constant to about one part in  $10^9$  over the sample volume. The longitudinal and transverse relaxation time constants  $T_1$  and  $T_2$  were measured using standard inversion-recovery and Carr-Purcell-Meiboom-Gill pulse sequences<sup>23</sup>, giving  $T_1 \approx 19$  and 25 seconds, and  $T_2 \approx 7$  and 0.3 seconds, respectively, for proton and carbon; these were much longer than required for our experiment, which finished in about 7 milliseconds.

The single most important source of errors in the experiments was the RF field inhomogeneity and pulse length calibration imperfections. A direct measure of this inhomogeneity is the  $\approx 200 \mu\text{s}$  time constant of the exponentially decaying envelope observed from applying a single pulse, as a function of pulse width. Including the population permutation sequence, about 7 pulses are applied to each nucleus, with a cumulative duration of  $\approx 70 - 100 \mu\text{s}$ .

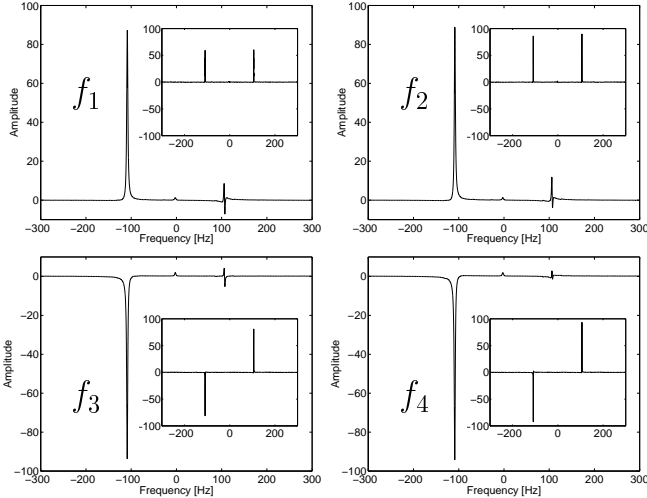


FIG. 2. Proton spectrum after completion of the D-J algorithm and a single read-out pulse  $X_A$ , with an effectively pure input state  $|00\rangle$  and with a thermal input state [Inset]. The low (high) frequency lines correspond to the transitions  $|00\rangle \leftrightarrow |10\rangle$  ( $|01\rangle \leftrightarrow |11\rangle$ ). The frequency is relative to 499755169 Hz, and the amplitude has arbitrary units. The spectrum is the Fourier transformed time varying voltage  $V(t)$ , induced in the pick up coil by the precession of spin  $A$  about  $-\mathbf{B}_0$ , at frequency  $\omega_A$ , after the read-out pulse  $X_A$ .  $V(t)$  is given by  $V(t) \approx V_0 \text{Tr} [e^{-i\hat{H}t} e^{-i\frac{\pi}{2}\hat{I}_x} \rho(0) e^{i\frac{\pi}{2}\hat{I}_x} e^{i\hat{H}t} \times (-i\hat{\sigma}_{xA} - \hat{\sigma}_{yA})]$ , where  $\hat{\sigma}_{\{x,y\}}$  are Pauli matrices, and  $\rho(0)$  is the density matrix of the state immediately before the readout pulse. By this convention, a spectral line for spin  $A$  is real and positive (negative) when spin  $A$  is  $|0\rangle$  ( $|1\rangle$ ) right before the  $X_A$  read-out pulse. Experiments were performed at Stanford University using an 11.7 Tesla Oxford Instruments magnet and a Varian <sup>UNITY</sup>Inova spectrometer with a triple-resonance probe.  $^{13}\text{C}$ -labeled  $\text{CHCl}_3$  was obtained from Cambridge Isotope Laboratories, Inc. [CLM-262].

The second most important contribution to errors is the low carbon signal-to-noise ratio, signal peak height/RMS noise  $\approx 35$ , versus  $\approx 4300$  for proton. The carbon signal was much weaker because the carbon gyromagnetic ratio is 4 times smaller, and the carbon receiver coil is mounted more remotely from the sample. Smaller contributions to errors came from incomplete relaxation between subsequent experiments, carrier frequency offsets, and numerical errors in the data analysis.

For this small-scale quantum computer, imperfections were dominated by technology, rather than by fundamental issues. However, NMR quantum computers larger than about 10 qubits will require creative new approaches, since the signal strength decays exponentially with the number of qubits in the machine, using current schemes <sup>24,25</sup>: for  $N$  spins the signal from the initial state  $00\dots 0$  is proportional to  $n_{00\dots 0} \propto NZ^{-N}$  where the single spin partition function  $Z \approx 2$  at high temperatures. Furthermore, coherence times typically decrease for larger molecules, while the average logic gate duration increases. Nevertheless, there is hope; for example, due to the ensemble nature of the NMR approach, one can infer the output result as long as a *distinguishable major-*

*ity* of the molecules reaches the correct final state. Creating an effective pure state is thus not always necessary, as we have demonstrated. Optical pumping and other cooling techniques can also be used to pre-polarize the sample to increase the output signal amplitude, since  $Z \approx 1$  at low temperatures. Quantum computation clearly poses an interesting and relevant experimental challenge for the future.

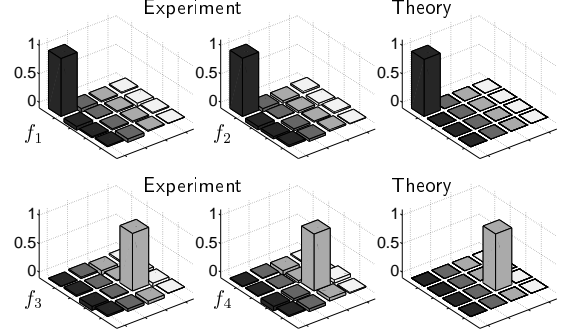


FIG. 3. Experimentally measured and theoretically expected deviation density matrices after completion of the D-J algorithm. The diagonal elements represent the normalized populations of the states  $|00\rangle, |01\rangle, |10\rangle$  and  $|11\rangle$  (from left to right). The off-diagonal elements represent coherences between different states. The magnitudes are shown with the sign of the real component; all imaginary components were small. The deviation density matrix was obtained from the integrals of the proton and carbon spectral lines, acquired for a series of 9 experiments with different read-out pulses for each spin (quantum state tomography <sup>24</sup>). The observed experimental non-idealities can be quantified as follows. In the experiments, the normalized pure-state population (ideally equal to 1), varied from 0.998 to 1.019. The other deviation density matrix elements (ideally 0), were smaller than 0.075 in magnitude. The relative error  $\epsilon$  on the experimental pure-state output density matrix  $\rho_{exp}$ , defined as  $\epsilon = \|\rho_{exp} - \rho_{theory}\| / \|\rho_{theory}\|$ , varied between 8 and 12%.

Note: during the preparation of this manuscript we became aware of a closely related experiment by J.A. Jones and M. Mosca at Oxford University <sup>26</sup>.

1. Deutsch, D. ‘Quantum Theory, the Church-Turing Principle and the Universal Quantum Computer,’ *Proc. R. Soc. Lond.*, **A**, **400**, 97-117 (1985).
2. Shor, P., ‘Algorithms for quantum computation: discrete logarithms and factoring,’ *Proc. 35<sup>th</sup> Ann. Symp. on Found. of Computer Science* (IEEE Comp. Soc. Press, Los Alamitos, CA, 1994) 124-134 .
3. Divincenzo, D. P., ‘Quantum computation,’ *Science* **270**, 5234, 255-261 (1995).
4. Lloyd, S., ‘Quantum-mechanical computers,’ *Scientific American* **273**, 44-50 (Oct. 1995).
5. Ekert, A. and Jozsa, R., ‘Quantum computation and Shor’s factoring algorithm,’ *Rev. of Mod. Physics* **68**, 3, 733-753 (1996).
6. Deutsch, D. and Jozsa, R., ‘Rapid solution of problems by quantum computation,’ *Proc. R. Soc. Lond.*, **A** **439**, 553-558 (1992).
7. Simon, D., ‘On the power of quantum computation,’ *Proc. 35<sup>th</sup> Ann. Symp. on Found. of Computer Science* (IEEE Comp. Soc. Press, Los Alamitos, CA, 1994) 116-123.
8. Grover, L. K., ‘Quantum computers can search arbitrarily large databases by a single query,’ *Phys. Rev. Lett.* **79**, 23, 4709-4012 (1997).
9. Unruh, W. G., ‘Maintaining coherence in quantum computers,’ *Phys. Rev. A* **51**, 2, 992-997 (1995).

10. Chuang, I. L., Laflamme, R., Shor, P. and Zurek, W. H., 'Quantum computers, factoring, and decoherence,' *Science* **270**, 5242, 1633-1635 (1995).
11. Landauer, R., 'Dissipation and Noise Immunity in Computation and Communication,' *Nature*, Vol. **335**, 779-784 (1988).
12. Landauer, R., 'Is Quantum Mechanics Useful?' *Phil. Trans. R. Soc. Lond. A*, **335**, 367-376 (1995).
13. Palma, G.M., Suominen, K.-A. and Ekert, A.K., 'Quantum Computers and Dissipation,' *Proc. R. Soc. Lond., A*, **452**, 567-584 (1996).
14. Monroe, C., Meekhof, D.M., King, B.E., Itano, W.M. and Wineland, D.J., 'Demonstration of a fundamental quantum logic gate,' *Phys. Rev. Lett.* **75**, 25, 4714-4717 (1995).
15. Turchette, Q. A., Hood, C.J., Lange, W., Mabuchi, H. and Kimble, H.J., 'Measurement of conditional phase shifts for quantum logic,' *Phys. Rev. Lett.* **75**, 25, 4710-4713 (1995).
16. Lloyd, S., 'A potentially realizable quantum computer,' *Science* **261**, 5128, 1569-1571 (1993).
17. Gershenfeld, N. and Chuang, I. L., 'Bulk spin-resonance quantum computation,' *Science* **275**, 5298, 350-356 (1997).
18. Cory, D. G., Price, M. D., Fahmy A. F. and Havel, T. F., 'Nuclear magnetic resonance spectroscopy: an experimentally accessible paradigm for quantum computing,' *Physica D*, in print; LANL E-print quant-ph/9709001.gov (1997).
19. Cory, D. G., Fahmy, A. F., and Havel, T. F., 'Ensemble quantum computing by NMR spectroscopy,' *Proc. Nat. Acad. Sci.* **94**, 1634-1639 (1997).
20. Cleve, R., Ekert, A., Macchiavello, C. and Mosca, M., *Proc. R. Soc. Lond., A*, **454**, 339-354 (1998); LANL E-print quant-ph/9708016.
21. Slichter, C. P., *Principles of Magnetic Resonance*. (Springer, Berlin, 1990).
22. Knill, E., Chuang, I. L. and Laflamme, R., 'Effective pure states for bulk quantum computation,' to appear in *Phys. Rev. A*, (1998); LANL E-print quant-ph/9706053.
23. Ernst, R. R., Bodenhausen, G. and Wokaun, A., *Principles of Nuclear Magnetic Resonance in One and Two Dimensions*. (Oxford University Press, Oxford, 1994).
24. Chuang, I. L., Gershenfeld, N., Kubinec, M. G. and Leung, D. W., 'Bulk quantum computation with nuclear magnetic resonance: Theory and experiment,' *Proc. R. Soc. Lond., A*, **454**, 447-467 (1998).
25. Warren, W. S., 'The Usefulness of NMR Quantum Computing,' *Science*, **277** 1688-1690 (1997).
26. Jones, T. F. and Mosca, M., 'Implementation of a Quantum Algorithm to Solve Deutsch's Problem on a Nuclear Magnetic Resonance Quantum Computer,' subm. to *J. of Chem. Phys.* (1998); LANL E-print quant-ph/9801027.

### *Acknowledgments*

We thank Alex Pines and Mark Kubinec for helpful discussions. This work was supported by DARPA under the NMRQC initiative. L.V. gratefully acknowledges a Francqui Fellowship of the Belgian American Educational Foundation and a Yansouni Family Fellowship.

Correspondence and requests for materials should be addressed to I.L. Chuang, electronic address [ichuang@almaden.ibm.com](mailto:ichuang@almaden.ibm.com)